AGU PUBLICATIONS

Paleoceanography

RESEARCH ARTICLE
10.1002/2014PA002644

Simulating Pliocene warmth and a permanent El Niño-like state: The role of cloud albedo

N. J. Burls[1] and A. V. Fedorov[1]

[1]Department of Geology and Geophysics, Yale University, New Haven, Connecticut, USA

Key Points:
- Cloud albedo changes may be a critical element of Pliocene climate
- Meridional SST gradient is a key in replicating the patterns of Pliocene warmth
- A robust ENSO despite the reduced mean east-west SST gradient

Correspondence to:
N. J. Burls,
natalie.burls@yale.edu

Citation:
Burls, N. J., and A. V. Fedorov (2014), Simulating Pliocene warmth and a permanent El Niño-like state: The role of cloud albedo, *Paleoceanography*, *29*, 893–910, doi:10.1002/2014PA002644.

Received 18 MAR 2014
Accepted 10 SEP 2014
Accepted article online 13 SEP 2014
Published online 6 OCT 2014

Abstract Available evidence suggests that during the early Pliocene (4–5 Ma) the mean east-west sea surface temperature (SST) gradient in the equatorial Pacific Ocean was significantly smaller than today, possibly reaching only 1–2°C. The meridional SST gradients were also substantially weaker, implying an expanded ocean warm pool in low latitudes. Subsequent global cooling led to the establishment of the stronger, modern temperature gradients. Given our understanding of the physical processes that maintain the present-day cold tongue in the east, warm pool in the west and hence sharp temperature contrasts, determining the key factors that maintained early Pliocene climate still presents a challenge for climate theories and models. This study demonstrates how different cloud properties could provide a solution. We show that a reduction in the meridional gradient in cloud albedo can sustain reduced meridional and zonal SST gradients, an expanded warm pool and warmer thermal stratification in the ocean, and weaker Hadley and Walker circulations in the atmosphere. Having conducted a range of hypothetical modified cloud albedo experiments, we arrive at our Pliocene simulation, which shows good agreement with proxy SST data from major equatorial and coastal upwelling regions, the tropical warm pool, middle and high latitudes, and available subsurface temperature data. As suggested by the observations, the simulated Pliocene-like climate sustains a robust El Niño-Southern Oscillation despite the reduced mean east-west SST gradient. Our results demonstrate that cloud albedo changes may be a critical element of Pliocene climate and that simulating the meridional SST gradient correctly is central to replicating the geographical patterns of Pliocene warmth.

1. Introduction

The surface of the Earth is characterized by large-scale horizontal temperature gradients, not only on land but within the world's oceans. Due to differential solar heating, partially mediated by atmospheric and oceanic poleward heat transport, strong meridional sea surface temperature (SST) gradients exist as temperatures decrease from the equator toward the poles. However, even along lines of homogeneous solar forcing, stark zonal SST gradients exist. The most pronounced basin-scale zonal SST gradients are found within the equatorial Pacific and Atlantic basins. Along the equator in the Pacific basin, mean SSTs range from over 29°C in the western warm pool region to about 23°C in the eastern cold tongue region. Associated with this east-west SST contrast is a zonal atmospheric circulation referred to as the Walker Cell [*Bjerknes*, 1969] wherein air rises over the warm SSTs in the west and descends over the cooler SSTs in the east.

What controls changes in these horizontal temperature gradients over geological time remains an important question within climate dynamics. In this context, the climate state of the early Pliocene epoch has attracted particular attention, especially as a potential analogue to present-day and future greenhouse-warming conditions. During the early Pliocene, the Earth, with a continental configuration similar to today, is thought to have experienced atmospheric CO_2 concentrations similar to the anthropogenically forced levels seen today. A recent compilation of available proxy data indicates that CO_2 levels during the early Pliocene were 50–100 p.p.m. greater than preindustrial levels (280 p.p.m.) [*Fedorov et al.*, 2013].

Paleoclimate records suggest that the early Pliocene was characterized by weak meridional as well as zonal SST gradients [*Chaisson and Ravelo*, 2000; *Wara et al.*, 2005; *Fedorov et al.*, 2006; *Ravelo et al.*, 2006; *Brierley et al.*, 2009; *Fedorov et al.*, 2013]. In particular, the pronounced cold tongue seen today in the eastern equatorial Pacific was 4–5°C warmer [*Wara et al.*, 2005; *Fedorov et al.*, 2006; *Dekens et al.*, 2007; *Lawrence et al.*, 2006; *Ford et al.*, 2012], and SSTs within subtropical coastal upwelling regions [*Herbert and Schuffert*, 1998;

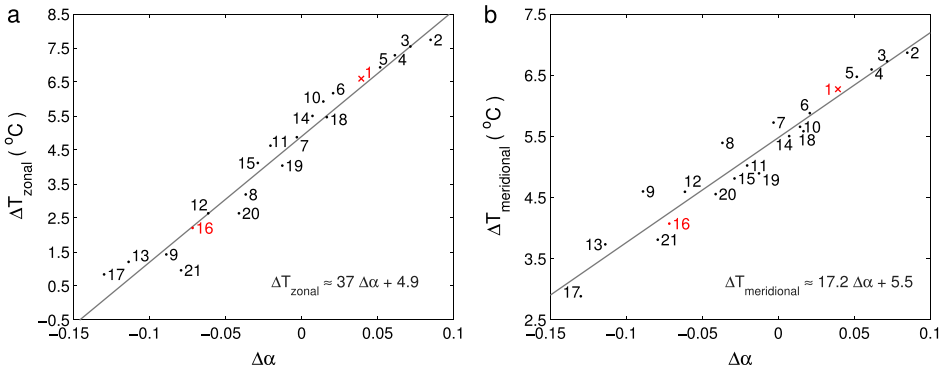

Figure 1. (a) East-west SST gradient along the equator (ΔT_{zonal}) and (b) mean meridional SST gradient ($\Delta T_{meridional}$) as a function of the meridional albedo gradient ($\Delta\alpha$) in the Pacific basin in the numerical experiments of *Burls and Fedorov* [2014] (the numbering of each experiment is consistent with their study). The exact definitions of these gradients are given in Table 1. This figure illustrates the tight linear relationship between zonal and meridional SST gradients and the meridional albedo gradient. These experiments were performed using a comprehensive climate model, CESM (T31 version); each run lasted 800 years. The albedo changes are achieved by modifying atmospheric liquid and ice water paths in the model's shortwave radiation code. Shown in red, 1 and 16 correspond to the control and Pliocene simulations, respectively.

LaRiviere et al., 2012; *Marlow et al.*, 2000; *Dekens et al.*, 2007; *Brierley et al.*, 2009] and the middle to high latitudes [*Lawrence et al.*, 2010; *LaRiviere et al.*, 2012] were substantially warmer than today (4–11°C). On the other hand, the warmest SSTs found within the tropical warm pool regions of the Pacific, Indian and Atlantic oceans appear to have changed very little over the last 5 million years [*Wara et al.*, 2005; *Karas et al.*, 2009; *Pagani et al.*, 2010; *Karas et al.*, 2011b; *Seki et al.*, 2012], which implies a reduction in meridional and zonal sea surface temperature gradients with respect to the present-day climate (for a recent review, see *Fedorov et al.* [2013]).

However, state-of-the-art coupled general circulation models (GCMs) forced with elevated CO_2 concentrations (400 p.p.m.) and, for example, reconstructed mid-Pliocene boundary conditions [*Haywood et al.*, 2007; *Lunt et al.*, 2010; *Dowsett et al.*, 2012, 2013] do not manage to reproduce the full extent of warming suggested by proxy data for the Pliocene epoch in the middle and high latitudes as well as the equatorial cold tongues and coastal upwelling regions. At the same time, these models produce too strong a warming in the oceanic warm pool regions as compared to the observations. As a result, the reduction in meridional and zonal sea surface temperature gradients and the general patterns of warming suggested by the paleodata are not captured by these simulations, even when resolving (to the best of our current knowledge) the effects associated with changes in CO_2, vegetation, ice sheets, and topography. Likewise, imposing changes in ocean gateways [*Maier-Reimer et al.*, 1990; *Cane and Molnar*, 2001; *Haug et al.*, 2001; *Lunt et al.*, 2008; *Molnar*, 2008; *Steph et al.*, 2010; *Zhang et al.*, 2012], such as an open Central American Seaway (CAS) or a more southerly position of Indonesia, is not sufficient to support the large-scale SST patterns during the Pliocene [*Zhang et al.*, 2012; *Fedorov et al.*, 2013]. On a more regional scale, the closure of the CAS has been invoked to explain a shoaling of the thermocline in the eastern Pacific from 4.8 to 4.0 by *Steph et al.* [2010] and *Ford et al.* [2012]. However, the relatively small changes in thermocline depth, resulting from realistic changes in the depth of the CAS imposed in climate models, have minor impacts on SST [*Zhang et al.*, 2012; *Fedorov et al.*, 2013].

Given these issues, how might a particular climate model simulate a Pliocene climate realistically? As reviewed by *Fedorov et al.* [2013], a number of physical processes unresolved or underestimated by these models might be the key to the Pliocene puzzle. This includes enhanced vertical mixing in the ocean [*Fedorov et al.*, 2010], atmospheric superrotation [*Tziperman and Farrell*, 2009], or different cloud properties—due perhaps to differences in the aerosol composition of the early Pliocene [*Martínez-Garcia et al.*, 2011] or an underestimated cloud response to extratropical and tropical warming [*Barreiro and Philander*, 2008; *Burls and Fedorov*, 2014]. The present study concentrates on the latter idea and simulates the early Pliocene-like climate by modifying the cloud properties that set cloud albedo.

A study by *Barreiro and Philander* [2008] has suggested that different low cloud properties may have played an important role in supporting Pliocene climate. In particular, they highlight that reduced extratropical

Table 1. Definitions of the Variables Shown in Figure 1, All for the Pacific Basin

Variable	Definition
Meridional SST gradient $\Delta T_{meridional}$	Difference between tropical (15°S–15°N) and extratropical (40–20°S, 20–40°N) Pacific SSTs
Zonal SST gradient ΔT_{zonal}	Difference between the maximum SST within the western equatorial Pacific (3°S–3°N, 140°E–165°E) and the minimum SST within the eastern equatorial Pacific (3°S-3°N, 250°E–275°E)
Meridional albedo gradient $\Delta\alpha$	Difference between extratropical (8–65°N and S) and tropical (8°S–8°N) albedo in the Pacific basin

cloud albedo can lead to a warming of the cold tongue and a reduction in the mean equatorial Pacific east-west SST gradient. However, in their coupled climate model (incorporating a simplified atmospheric model), a relatively modest reduction of the east-west gradient, on the order of 1°C, occurs in response to a very large, 50% reduction in extratropical low-cloud cover. A subsequent study [*Burls and Fedorov*, 2014] has shown, however, that it is not just the extratropical clouds, but rather the entire meridional gradient in cloud albedo that controls the zonal SST gradient along the equator.

In particular, *Burls and Fedorov* [2014] argue that a reduced meridional gradient in cloud albedo (reduced extratropical and increased tropical albedo relative to the present day) could maintain weaker meridional and zonal temperature gradients. Specifically, lower extratropical cloud albedo increases the amount of shortwave radiation reaching the ocean surface raising the temperature of water subducted in the downwelling regions of the wind-driven shallow subtropical cells (STCs) [*McCreary and Lu*, 1994; *Gu and Philander*, 1997]. With the STCs controlling thermocline waters in the tropics, this extratropical warming results in a weaker meridional temperature gradient and translates into the upwelling of warmer subsurface water in the equatorial and coastal upwelling regions, decreasing the zonal SST gradient. At the same time, increased tropical albedo acts to reduce the flux of heat into the ocean along the equator regulating warm pool temperatures and hence the meridional and zonal gradients. Changes in the gradient in cloud albedo between the tropics and midlatitudes therefore present a mechanism for long-term changes in the east-west tropical

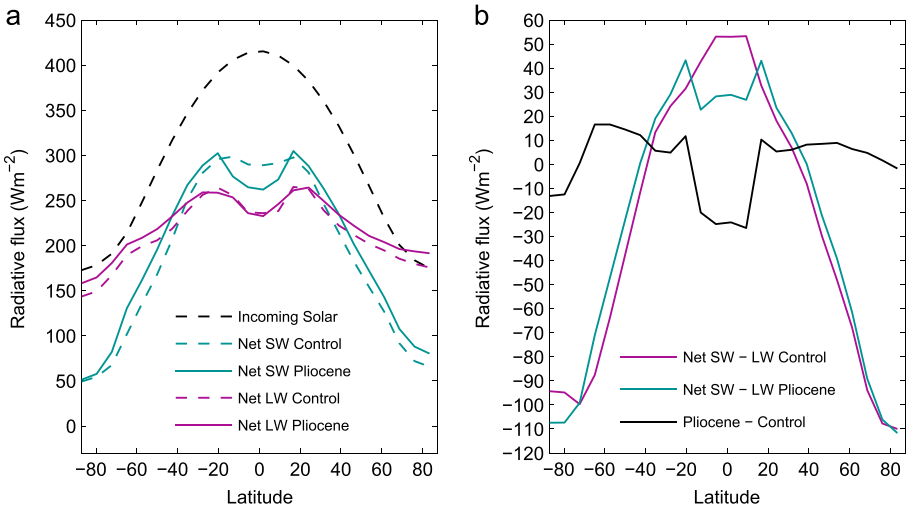

Figure 2. (a) Zonally averaged net (incoming minus reflected) shortwave and longwave fluxes at the top of the atmosphere for the preindustrial control and the Pliocene experiment (experiments 1 and 16 in Figure 1). The latter simulation with modified cloud albedo is the experiment that most closely resembles early Pliocene conditions. (b) The net top-of-the-atmosphere radiative budgets (shortwave minus longwave) and their difference for the two experiments. The difference (black line) represents the effective radiative forcing for the early Pliocene experiment. This forcing results from the imposed atmospheric water path modifications such that extratropical (poleward of 8°N and S) cloud albedo has reduced by 0.04 and tropical (8°S–8°N) cloud albedo has increased by 0.06.

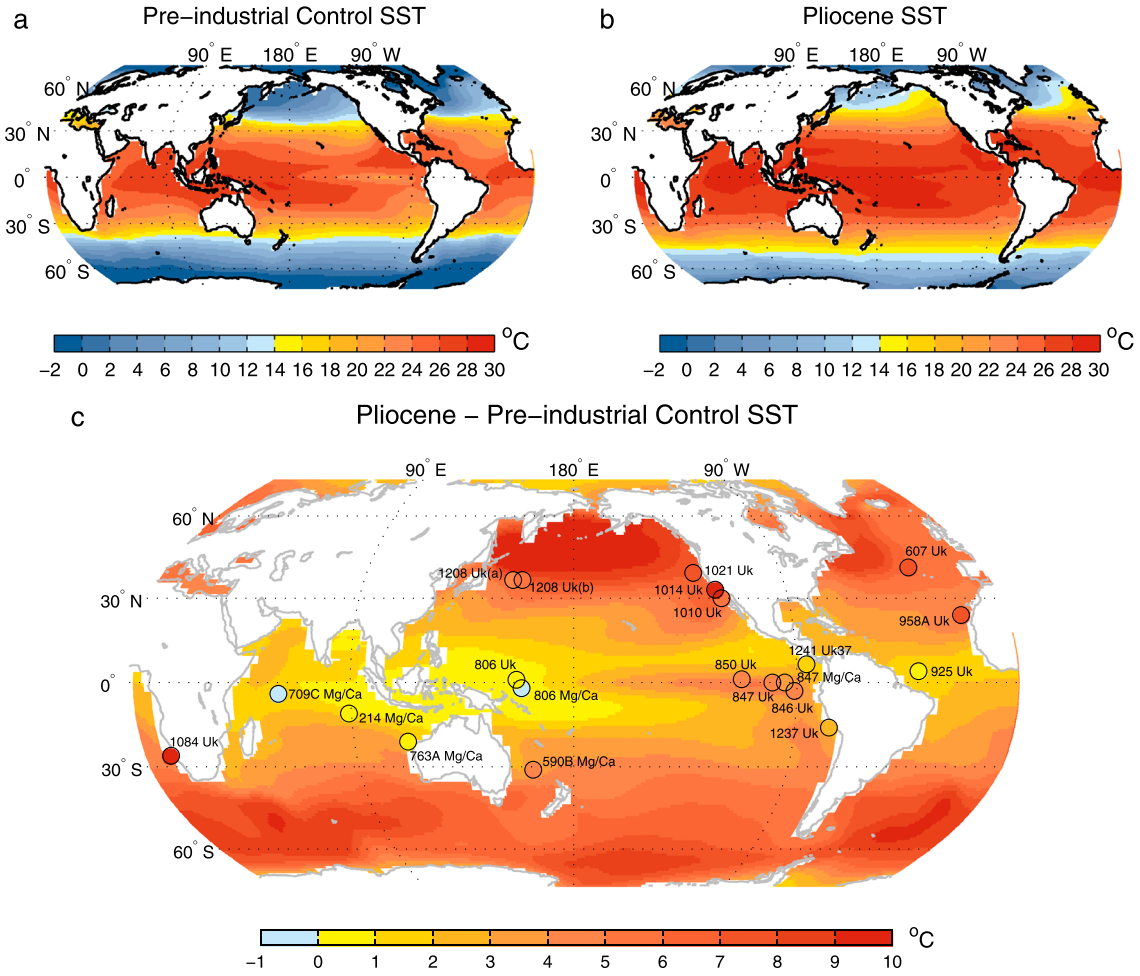

Figure 3. Mean SST fields for (a) the preindustrial control and (b) the early Pliocene experiments and (c) the corresponding SST anomalies for the Pliocene experiment relative to the control. Superimposed on these SST anomalies are the observed differences between modern and early Pliocene SST estimates at available sites; see Table 2 as well as *Fedorov et al.* [2013] for details on the proxy records and how they were analyzed.

Pacific SST gradient. This cloud albedo control on the vertical structure of the tropical ocean and the strength of meridional and zonal gradients can also be understood from a heat budget perspective [*Boccaletti et al.*, 2004; *Fedorov et al.*, 2004].

In this study, we build on the work of *Burls and Fedorov* [2014] and establish, within a state-of-the-art fully coupled climate model, the magnitude and spatial structure of the latitudinal cloud albedo changes required to reproduce a change in the global ocean surface temperature structure that closely resembles the proxy data. We emphasize that the specified modifications in the cloud properties controlling albedo (atmospheric water path, see next section) are strictly zonal, but the response of the climate system varies in both latitude and longitude and is not necessarily hemispherically symmetric. In other words, all elements of the climate system are allowed to evolve freely under the imposed changes, which makes this approach different from flux corrections [e.g., *Manabe and Stouffer*, 1988]. While the imposed changes in the albedo of a cloud when it forms in the model are purely hypothetical, possible causes could include, for example, unresolved cloud feedbacks under greenhouse warming or changes in atmospheric aerosol concentrations [e.g., *Kiehl and Shields*, 2013; *Kump and Pollard*, 2008].

The structure of this paper is as follows. In section 2 we describe the approach employed to perturb the albedo of low-level extratropical clouds as well as the albedo of both low and high clouds within the tropics. Our results demonstrate that a relatively moderate reduction in the meridional gradient in cloud albedo can sustain reduced meridional and zonal gradients in sea surface temperature (section 3), an expanded warm pool in the ocean (section 3), and weaker Hadley and Walker circulations in the atmosphere (section 4).

Table 2. ODP Sites and Proxy Data Used for the Global Model-Data SST Comparison in Figure 3c[a]

Site	Latitude	Longitude	Method	Observed Pliocene Temperature Anomaly (°C)	Simulated Pliocene Temperature Anomaly (°C)	References
ODP 806	0°N	159°E	Mg/Ca; Uk'37	−0.7; 0.8	0.6	*Wara et al.* [2005]; *Pagani et al.* [2010]
ODP 709C	4°S	61°E	Mg/Ca	−1.5	1.4	*Karas et al.* [2011b]
ODP 763A	21°S	112°E	Mg/Ca	0.5	3.1	*Karas et al.* [2011b]
ODP 214	11°S	89°E	Mg/Ca	0.1	1.9	*Karas et al.* [2009]
ODP 925	4°N	43°W	Uk'37	0.9	1.7	*Pagani et al.* [2010]
ODP 1241	6°N	86°W	Uk'37	1.4	2.1	*Seki et al.* [2012]
ODP 846	3°S	91°W	Uk'37	4.4	4	*Liu and Herbert* [2004]; *Lawrence et al.* [2009]
ODP 847	0°N	95°W	Mg/Ca; Uk'37	3.9; 4.1	4.5	*Wara et al.* [2005]; *Fedorov et al.* [2006]; *Dekens et al.* [2007]
ODP 850	1°N	110°W	Uk'37	4.3	5	*Zhang et al.* [2014]
ODP 1237	16°S	76°W	Uk'37	2.6	2.9	*Dekens et al.* [2007]
ODP 1010	30°N	118°W	Uk'37	5.8	5.9	*LaRiviere et al.* [2012]
ODP 1014	33°N	120°W	Uk'37	10.7	6.7	*Dekens et al.* [2007]
ODP 958A	24°N	20°W	Uk'37	7.9	4.5	*Herbert and Schuffert* [1998]
ODP 1084	26°S	13°E	Uk'37	10.7	4.6	*Marlow et al.* [2000]
ODP 590B	31°S	163°E	Mg/Ca	4.1	3.8	*Karas et al.* [2011a]
ODP 1208	37°N	158°E	Uk'37	4.7; 5.9	6.5	*LaRiviere et al.* [2012]; *Pagani et al.* [2010]
ODP 1021	39°N	128°W	Uk'37	7.4	7	*LaRiviere et al.* [2012]
ODP 607	41°N	33°W	Uk'37	7.4	5.6	*Lawrence et al.* [2010]

[a]Observed early Pliocene SST anomalies are defined as the average difference in the available data at each site between the intervals 4–5 Ma and 0–0.5 Ma. Each time series is interpolated to a constant spacing of 2 kyr prior to analysis and, if the data does not span 0–0.5 Ma, present-day annual mean SST values are used. An alternative way to estimate these anomalies is to use only interglacial temperatures within the two time intervals. However, the latter method gives values that differ only by 0.5–1°C from those computed in this paper (see Figure S1 in *Fedorov et al.* [2013]), less than the relevant error bars. Finally, simulated Pliocene anomalies are given by the difference between the Pliocene and control simulations.

Within this simulated climate state, we investigate the key differences between the early Pliocene and modern climate, including differences in the ocean vertical thermal structure, surface wind, precipitation, and the El Niño-Southern Oscillation (ENSO, section 5). We conclude with a discussion in section 6.

2. Experimental Design

The coupled climate model used in this study is the National Center for Atmospheric Research, Community Earth System Model (CESM) version 1.0.4. The two experiments analyzed, control and Pliocene-like, make use of the T31 gx3v7 configuration, wherein the atmospheric component has a spectral truncation of T31, and the oceanic component has a resolution varying from about 3° near the poles to 1° at the equator.

Using the same model, *Burls and Fedorov* [2014] systematically explore the robustness of our theoretical understanding of what controls the mean east-west SST gradient in the equatorial Pacific under a wide range of climates. Spatial variations in cloud albedo are used as a means to modify the meridional gradient in local equilibrium SST and the required poleward ocean heat transport. To change the meridional gradient

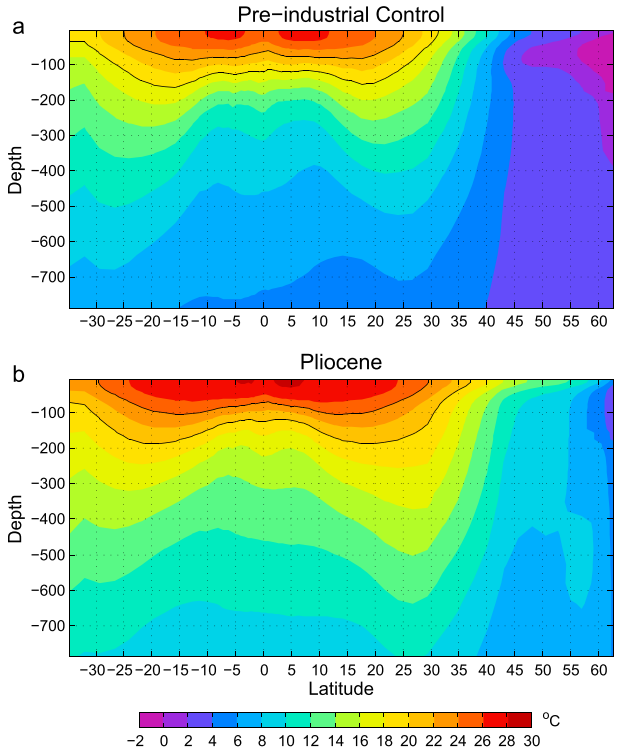

Figure 4. The zonal mean temperature structure of the Pacific Ocean for (a) the preindustrial control and (b) the early Pliocene experiment. In the Pliocene experiment the subduction of warmer subtropical surface water maintains warmer thermocline waters in coastal and equatorial upwelling regions relative to the preindustrial control. The solid black contours highlight the subduction of subtropical waters into the thermocline: 18–22°C for the preindustrial control versus 20–24°C for the Pliocene experiment.

in cloud albedo within each numerical experiment, the optical properties of clouds are changed by modifying the atmospheric liquid and ice water paths, but only in the shortwave radiation scheme of the model. Changes in the atmospheric liquid water path affect the albedo of highly reflective low stratus clouds when they form in the model, while changes in the ice path also affect the albedo of high clouds. The liquid water and ice paths remain unaltered in the longwave radiation scheme allowing the system to freely adjust its longwave forcing. The experiments differ in the magnitude and meridional extent of changes in the atmospheric water path, and hence imposed changes in local cloud albedo, resulting in a range of experiments supporting a variety of planetary albedos and meridional albedo contrasts as shown in Figure 1. Modifying the atmospheric water path serves as an efficient and relatively straightforward way of imposing cloud albedo changes within a comprehensive coupled climate model. We emphasize however that these changes could be realized by changes in a number of cloud properties in addition to liquid and ice water content, e.g., cloud lifetime, particle concentration, and size. For further details on how the atmospheric albedo changes were imposed, we refer the reader to *Burls and Fedorov* [2014].

The main result emerging from Figure 1 is that the gradient in cloud albedo between the tropics and midlatitudes within the Pacific basin ($\Delta\alpha$) sets the mean east-west equatorial Pacific SST gradient (ΔT_{zonal}). A strong relationship also exists between the meridional SST gradient ($\Delta T_{\text{meridional}}$) and $\Delta\alpha$. As the meridional albedo gradient is varied from approximately −0.15 to 0.1 within the experiments conducted, the equatorial east-west SST gradient (Figure 1a) and meridional SST gradient (Figure 1b) within the Pacific basin reduces from 7.5°C to below 1°C and from 7°C to below 3°C, respectively. This close dependence can be accounted for by an energy balance model incorporating the essential dynamics of the warm pool, cold tongue, and Walker circulation complex [*Burls and Fedorov*, 2014].

Thus, the results in Figure 1 demonstrate that a reduced meridional cloud albedo gradient can sustain weaker SST contrasts in low latitudes. The next step is to choose a climate state among the experiments that best reproduces early Pliocene conditions. In choosing this state we apply just two criteria: the climate state should have a meridional SST gradient similar to that observed for the early Pliocene and it should maintain relatively unchanged SSTs in the warm pool region. While several simulations come close to satisfying these criteria (within the data uncertainty), experiment 16 appears to give the best match. For example, while experiments 9 and 21 maintain meridional SST gradients similar in magnitude to experiment 16 (Figure 1b), their warm pool temperatures are more than 2°C above or below the control temperature, respectively. In experiment 9 the reduction in extratropical albedo, and hence global albedo, is too large resulting in a climate much warmer than the Pliocene (the global mean surface temperature is 12°C greater than the preindustrial control). In experiment 21 the imposed increase in tropical and subtropical albedo is too extreme, leading to tropical SSTs colder than the control. As discussed in the next section, by imposing these two criteria, we manage to reproduce a climate state with SSTs and subsurface ocean temperatures closely resembling available proxy data for the early Pliocene in different locations of the global ocean (including

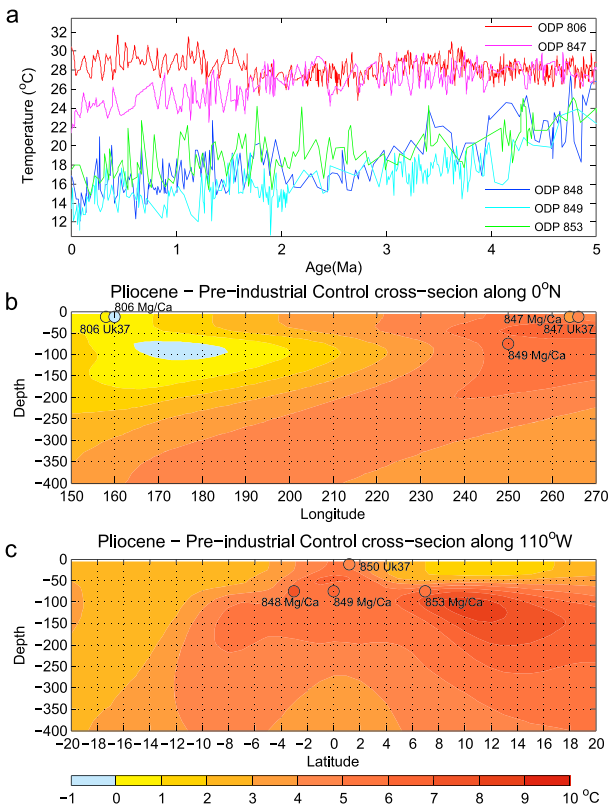

Figure 5. (a) Proxy SST records in the western and eastern equatorial Pacific (ODP sites 806 and 847) and subsurface temperatures in the eastern equatorial Pacific (ODP sites 848, 849, and 853). Note significant warming in the east but relatively stable surface temperatures in the west during the early Pliocene. (b) East-west (along 0°N) and (c) north-south (along 110°W) transects showing ocean temperature changes between the preindustrial control and the early Pliocene experiments. Superimposed are the observed differences between modern and early Pliocene temperatures based on the available data. The details for each proxy records and how they were analyzed are given in Table 3. The depth of the three subsurface sites is set at 75 m, reflecting a feasible habitat range of 50–100 m for the foraminifer species used in the analysis [*Ford et al.*, 2012].

the reduced equatorial east-west SST gradient in the Pacific). Therefore, from here on we will refer to this experiment as the early Pliocene experiment.

Each T31 experiment in *Burls and Fedorov* [2014] was run for 800 years. This time scale is of sufficient length to allow for the adjustment of the shallow tropical and subtropical oceanic circulations, and hence tropical and subtropical SSTs. However, this time scale is only marginally sufficient for the adjustment of the deep ocean—after 800 years the model top-of-the-atmosphere (TOA) imbalance was 0.45 W m^{-2}, indicating that the ocean was still gaining heat. To reduce this imbalance, we have extended the early Pliocene-like simulation to 3000 years. Extending the simulation to near equilibrium was necessary for the purposes of this study as it assesses global SST changes, unlike *Burls and Fedorov* [2014] which focuses on tropical and subtropical SST changes. In the present study, the TOA imbalance averaged over the last 500 years of each simulation reaches only 0.02 W m^{-2} for the control and −0.04 W m^{-2} for the Pliocene experiment, indicating that the Earth's climate system has approximately reached a steady state. For the Pliocene experiment the top of model imbalance gradually decreased from 0.45 W m^{-2} after 800 years to 0.1 W m^{-2} after 1500 years, reaching the same order of magnitude as the control simulation after 2000 years.

The simulated TOA radiation forcing required to shift from the preindustrial climate to the Pliocene-like conditions is shown in Figure 2. This radiation forcing arises due to the imposed modifications in atmospheric water path that amount to a decrease in extratropical (8–90°N and S) albedo of 0.04 and an increase in tropical albedo (8°S–8°N) of 0.06. The imposed changes in cloud properties results on average in a 5% and 3.3% increase in the extratropical, top of the atmosphere, net shortwave and longwave forcing, respectively, and a 9% decrease in the tropical shortwave forcing with a relatively small 0.5% decrease in tropical longwave forcing (Figure 2). The imposed changes also result in a net decrease in global albedo of 0.029, leading to a 5.5°C increase in global mean surface temperature between the preindustrial control and the early Pliocene experiment. This global mean surface temperature is slightly greater than the 4°C difference obtained by *Brierley and Fedorov* [2010] who used an atmospheric model forced by a hypothetical SST reconstruction with relaxed SST gradients to simulate the early Pliocene. It is also higher than the 2–3°C model based estimates for the mid-Pliocene [*Haywood and Valdes*, 2004; *Lunt et al.*, 2010].

Since we aimed to isolate the potential effect of cloud albedo variations on Pliocene climate, the Pliocene simulation does not explicitly take into consideration the relatively uniform warming that would result from elevated CO_2 levels—Pliocene estimates are 50–100 p.p.m. greater than preindustrial levels (280 p.p.m.), though there is large uncertainty in these values [*Fedorov et al.*, 2013]. However, the potential effects of increased CO_2 levels are partially mimicked in the Pliocene-like experiment by the imposed albedo

Table 3. ODP Sites and Proxy Data Used for the Equatorial Pacific Model-Data Comparison in Figure 5[a]

Site	Latitude	Longitude	Method	Observed Pliocene Temperature Anomaly (°C)	Simulated Pliocene Temperature Anomaly (°C)	References
ODP 806	0°N	159°E	Mg/Ca; Uk'37	−0.7; 0.8	0.6	*Wara et al.* [2005]; *Pagani et al.* [2010]
ODP 847	0°N	95°W	Mg/Ca; Uk'37	3.9; 4.1	4.5	*Wara et al.* [2005]; *Fedorov et al.* [2006]; *Dekens et al.* [2007]
ODP 850	1°N	110°W	Uk'37	4.3	5	*Zhang et al.* [2014]
ODP 848	3°S	110°W	Mg/Ca	7.3	5.3	*Ford et al.* [2012] with *Mohtadi et al.* [2011] temperature calibration
ODP 849	0°N	110°W	Mg/Ca	6.3	5.5	*Ford et al.* [2012] with *Mohtadi et al.* [2011] temperature calibration
ODP 853	7°N	110°W	Mg/Ca	5.2	6.2	*Ford et al.* [2012] with *Mohtadi et al.* [2011] temperature calibration

[a]Temperature anomalies are defined as described in the caption for Table 2.

reduction in middle to high latitudes. The two radiative forcings are not exactly equivalent, but the SST response to a reduction in cloud albedo poleward of 35°N and S is seen to have a similar spatial structure as the response to a moderate global CO_2 increase (for example, see Figures 5 and S11 in *Fedorov et al.* [2013] comparing the effects of a 100 p.p.m. CO_2 increase versus reduced cloud albedo). Including CO_2 forcing would decrease the reduction in extratropical albedo needed to warm the middle to high latitudes and the temperature of water subducted in the downwelling regions of the subtropical cells.

In the following sections we will contrast the early Pliocene simulation against the preindustrial control in detail. The analysis presented is based on the last 500 years of each experiment (except for the ENSO analysis in section 5 where the last 143 years is used to facilitate comparison with observations).

3. Simulated SST Patterns and Ocean Thermal Structure in the Early Pliocene

Figure 3 compares the mean SST field for the early Pliocene experiment with that of the control. Consistent with the SST field reconstruction of *Brierley et al.* [2009], the early Pliocene simulation yields an expanded warm pool with ocean surface temperatures greater than 26°C extending poleward of 20°N and S. Maximum SSTs within the warm pool increase only slightly ($\leq$1°C, see Figure 3c). The cold tongue on the other hand has all but disappeared (Figure 3b), with warm tropical SSTs ($\geq$ 26°C) extending all the way across the equatorial Pacific.

SST differences in particular locations are further quantified in Figure 3c, in which superimposed circles directly compare the observed early Pliocene SST anomalies (relative to the modern SSTs) to those simulated by the climate model. The early Pliocene experiment has managed to capture the structural change in global SSTs that occurred between modern conditions and the early Pliocene [*Fedorov et al.*, 2013]. While SSTs within the tropical warm pools have hardly changed ($-1°C \leq \Delta SST \leq 1°C$), SSTs within equatorial upwelling regions have increased by 3–5°C leading to a significant reduction in the zonal SST gradient along the equator. Mirroring the proxy data, the largest changes in simulated SSTs (5–9°C) occur within the subtropical coastal upwelling regions and the midlatitudes, which is consistent with a substantial reduction in the meridional SST gradient. Conventional Pliocene simulations, without modifications in cloud physics, are unable to capture these features of Pliocene climate [*Dowsett et al.*, 2013].

SST changes within subtropical coastal upwelling regions are somewhat underestimated by the model in comparison to the data, presumably because of the relatively course resolution of the climate model. The model does simulate a weakening of the alongshore winds, reducing the coastal upwelling (see the next section), but the warming of SSTs in response is relatively weak.

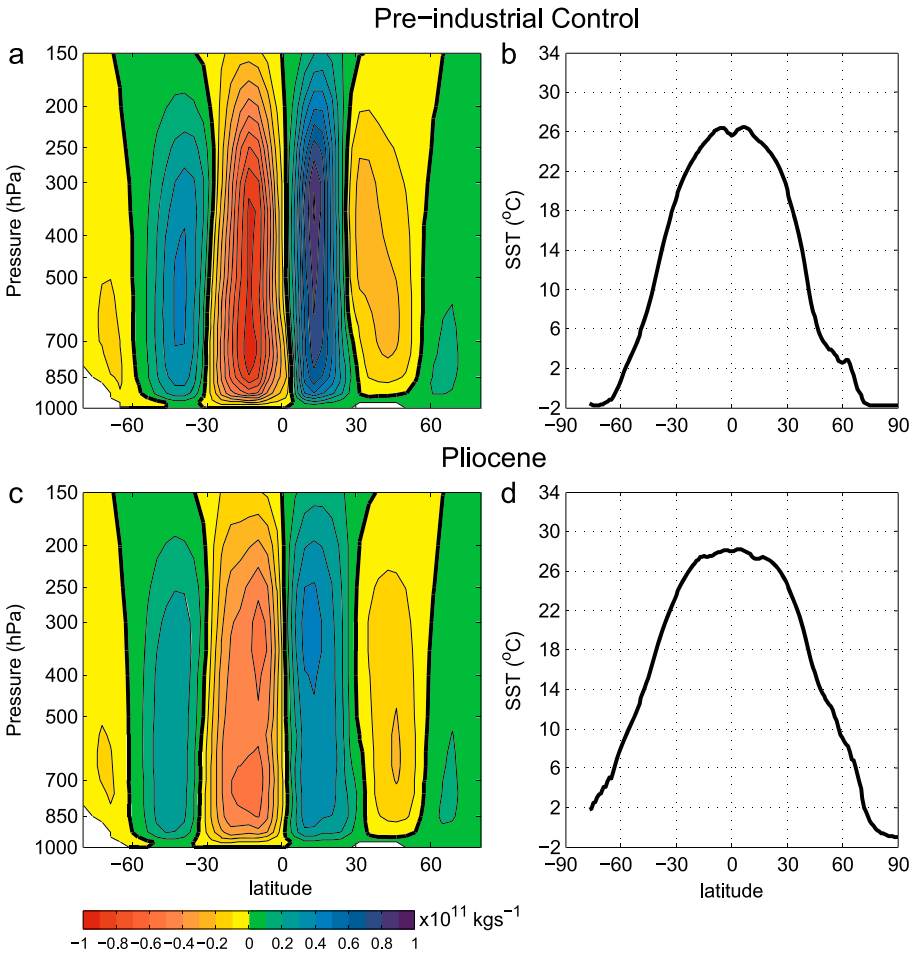

Figure 6. (a) The zonal mean stream function and (b) zonal mean SST for the preindustrial control experiment; (c and d) the same climatic variables for the early Pliocene experiment. In response to an expanded tropical warm pool and reduced meridional SST gradients, the early Pliocene experiment sustains a weaker Hadley circulation [also see *Brierley et al.*, 2009].

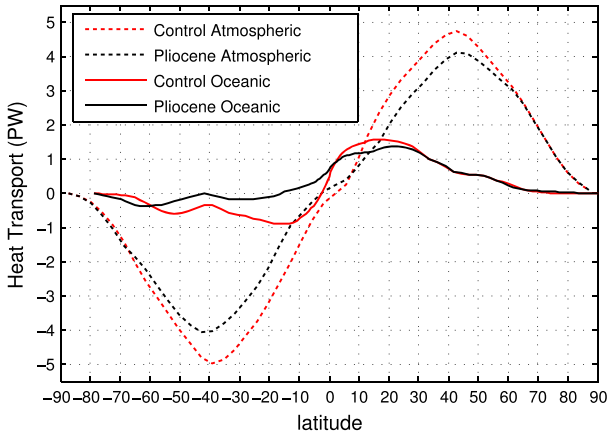

Figure 7. A comparison of the global northward atmospheric (dashed) and oceanic (solid) heat transport between the preindustrial control (red) and the early Pliocene (black) experiments. The reduced meridional cloud albedo gradient supports weaker meridional SST gradients, a weaker Hadley circulation, and hence reduced poleward atmospheric and oceanic heat transport in the early Pliocene experiment.

A change in the thermal structure of the ocean appears to be a fundamental factor contributing to the distinctly different global sea surface temperature pattern within the early Pliocene experiment. As shown in Figure 4, the imposed reduction in extratropical cloud albedo leads to increased ocean temperatures in the subduction regions of the subtropical cells, resulting in the warmer thermocline water being upwelled in coastal and equatorial upwelling regions.

Figure 5 provides additional evidence in support of the hypothesis that a change in the thermal structure of the ocean played a major role in maintaining the structurally different SST field of the early Pliocene [*Philander and*

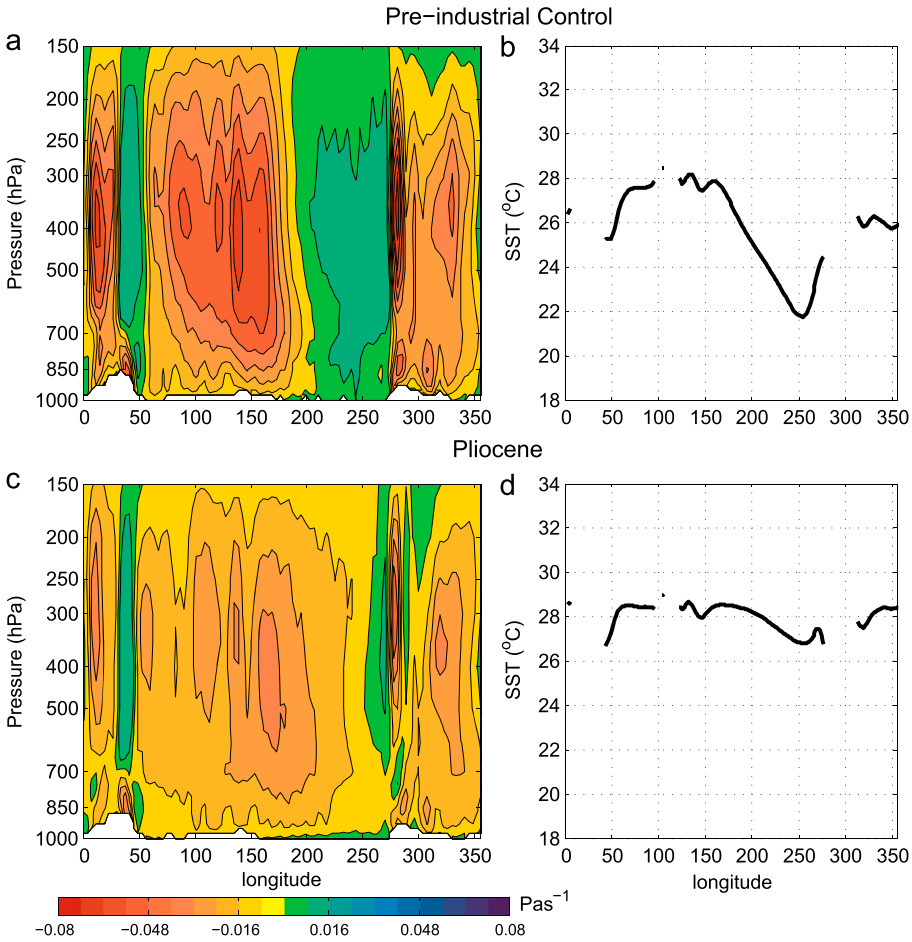

Figure 8. (a) Pressure velocity anomalies along the equator indicating mean vertical flow in the Walker circulation and (b) equatorial SSTs for the preindustrial control experiment; (c and d) the same climatic variables for the early Pliocene experiment. Pressure velocity anomalies are computed as deviations from the zonal mean values and are averaged between 8°S and 8°N; SSTs are averaged between 1.5°S and 1.5°N. In the control experiment the Walker cell in the Pacific is seen as large negative anomalies around 150°E (ascent, red) and positive anomalies (subsidence, green) around 250°E. While warm-pool temperatures in the western Pacific in the Pliocene experiment remain near 28°C, temperatures in the middle of the eastern Pacific cold tongue have warmed by 4°C, reducing the east-west equatorial SST gradient and the Walker circulation substantially.

Fedorov, 2003; *Fedorov et al.*, 2006]. The warming of thermocline waters in the Pliocene epoch, captured within subsurface temperature records along 110°W in the eastern equatorial Pacific [*Ford et al.*, 2012], is associated with a substantial increase in surface temperatures in the eastern but not the western Pacific (Figure 5a). The Pliocene simulation, with the imposed latitudinal cloud albedo modifications, has managed to reproduce the observed surface and subsurface temperature changes along the equator quite realistically, including a 3–6°C warming in the eastern Pacific and a below 1°C SST increase in the western Pacific (Figure 5b). Warmer waters, subducted in the extratropics (Figure 4b) and transported by the STCs and the Equatorial Undercurrent, maintain this warming in the eastern equatorial Pacific.

Figure 5c further compares the simulated changes in the thermal structure of the ocean along 110°W with available subsurface temperature estimates from *Ford et al.* [2012]. The model simulation suggests a broad warming along this longitude, on the order of 5–8°C, at depths of 50–300 m. This warming is attributed to both the warmer Equatorial Undercurrent source waters subducted in the STCs and reduced Ekman pumping due to weaker trades (also see section 4).

The maximum warming occurs at about 10°N between 100 and 150 m. This feature is due to a change in wind stress curl and Ekman pumping between the two experiments, associated with changes in the

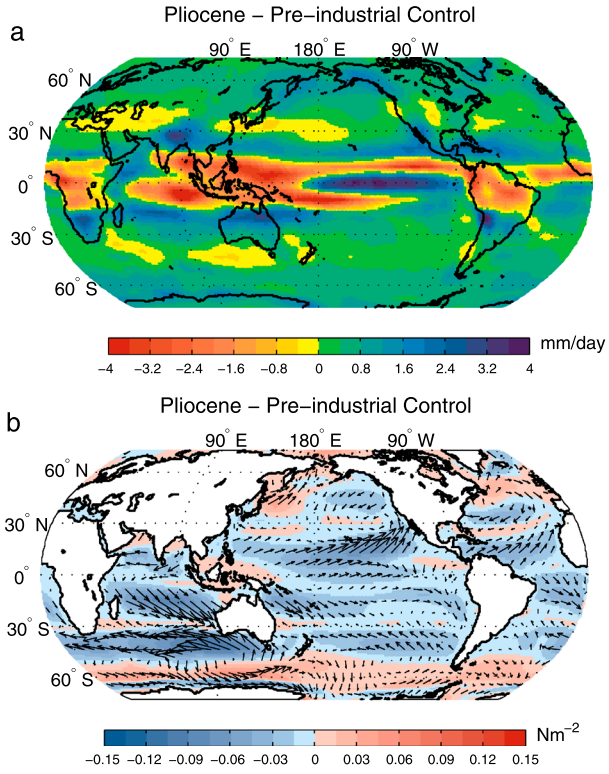

Figure 9. Simulated changes in the annual mean (a) precipitation rates and (b) ocean surface wind stress during the early Pliocene relative to the preindustrial control experiment. Arrows and colors in Figure 9b indicate wind stress vectors and magnitude, respectively. Consistent with a weakening of the Hadley and Walker circulations, the trade winds within the early Pliocene experiment weaken, whereas precipitation is reduced in convective regions and enhanced in areas dominated by subsidence. The amplified high-latitude warming seen in the early Pliocene experiment results in the poleward shift of the midlatitude westerlies. Also, note the weakening of meridional winds along the basin eastern boundaries (over the coastal upwelling regions) associated with a weakening of the subtropical high-pressure zones.

seasonal migration of the Intertropical Convergence Zone (ITCZ). The ITCZ gives rise to cyclonic wind stress curl which supports a doming of the oceanic thermocline beneath it and therefore cool temperatures just below the mixed layer. However, low wind speeds in the region of the ITCZ maintain warm SSTs by suppressing the entrainment of this cold subsurface water into the surface mixed layer. As a result, a sharp vertical gradient exists in ocean temperatures beneath the mean position of the ITCZ. In the early Pliocene simulation, the disappearance of cold SSTs south of the equator allows the ITCZ to cross the equator more readily and therefore Ekman pumping north of the equator is suppressed. This shift between the preindustrial control and the Pliocene experiments results in a relatively small temperature change of 1–3°C above 50 m, a 3–5°C change between 50 and 75 m and a 5–8°C change between 75 and 100 m.

Within data uncertainty, the simulated subsurface temperature changes are generally consistent with the proxy data indicating that ocean temperatures were 4–6°C warmer between 50 and 100 m. Some differences are probably due to the crudeness of the imposed forcing or, especially at the northern site, due to uncertainty in the depth of the habitat of the foraminifera species used—there exists a strong vertical gradient in temperature and small changes in this depth can result in a large temperature signal.

Note that several new records, based on the TEX86 temperature proxy, have recently been generated for sites in the western and eastern tropical Pacific [*Seki et al.*, 2012; *Zhang et al.*, 2014]. Although generally consistent with the simulated SST changes, these Tex86 data have not been included in the comparison of Figure 3c because they suffer from cold biases over the Pleistocene-Pliocene interval and may not strictly represent SST changes in the equatorial band [*Seki et al.*, 2012; Ravelo et al., Reconfirming permanent El Niño-like conditions of the early Pliocene: A comment on the Zhang et al. 2014 study, submitted to *Science*, 2014]. For example, in the eastern equatorial Pacific, at ODP sites 850 [*Zhang et al.*, 2014] and 1241 [*Seki et al.*, 2012], the TEX86 data produce temperatures up to 5°C colder than other SST proxies over the past 5 million years. Such biases most likely reflect the fact that in the equatorial region the TEX86 proxy describes depth-integrated temperature rather than SST. Consequently, some of the trends seen in TEX86 could be related to subsurface temperature changes (Figure 5). In fact, the cold bias in TEX86 at sites 850 and 1241 is stronger in the Pleistocene than in the Pliocene—the bias decreases with the warmer subsurface temperatures characteristic of the Pliocene [*Ford et al.*, 2012]. One could also note our modeling results for the western equatorial Pacific (Figure 5b)—while SSTs in the west hardly change, the subsurface warming is much stronger due to the warming of the Equatorial Undercurrent source waters.

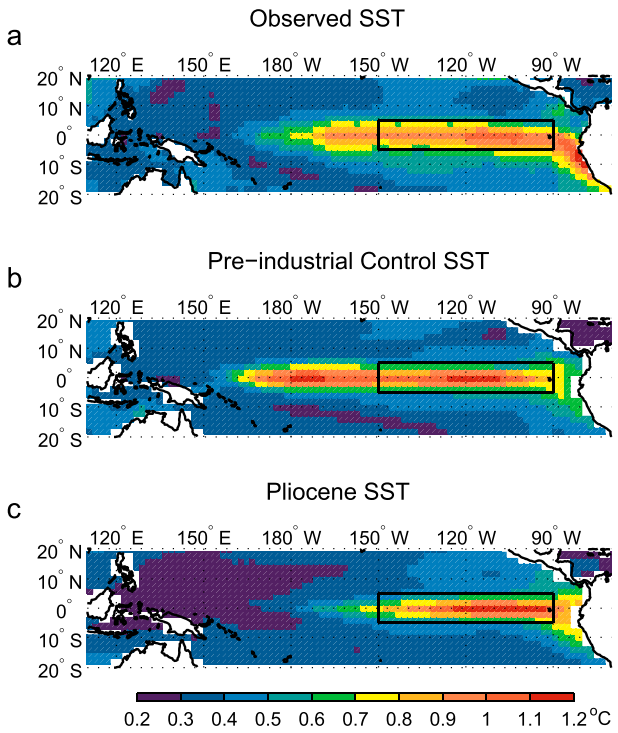

Figure 10. SST variance (in °C) as a function of longitude and latitude for (a) observations and the (b) preindustrial control and (c) early Pliocene experiments. The observed record is based on Hadley Centre Sea Ice and Sea Surface Temperature data set (HadISST) [*Rayner et al.*, 2003] spanning from January 1870 to December 2012. Figures 10b and 10c are based on the last 143 years of the numerical simulations. The boxes indicate the boundaries of the Niño3 region.

4. Atmospheric Circulation: Hadley and Walker Cells, Wind, and Precipitation Changes

As expected, the transition to weak SST gradients in the early Pliocene experiment is accompanied by large changes in atmospheric circulation. Accordingly, the reduction of the meridional gradient leads to a weakening of the Hadley circulation, consistent with the study of *Brierley et al.* [2009]. Figure 6 compares the zonal mean SST structure and corresponding atmospheric meridional stream function between the preindustrial and Pliocene experiments. The increased meridional extent of the tropical warm pool (Figure 6d versus Figure 6b) acts to reduce the meridional SST gradient within the tropics and subtropics supporting weaker Hadley circulation in the Pliocene experiment (Figure 6c versus Figure 6a).

The weaker meridional SST gradients and Hadley circulation result in reduced meridional atmospheric heat transport as illustrated by Figure 7. Since oceanic circulation in the tropical Pacific is largely wind-driven, oceanic heat transport weakens as well, leading to the reduction of the total poleward heat transport. We emphasize, however, that the system remains energetically balanced since the reduction in the total poleward heat transport is required by the imposed forcing (see top-of-the-atmosphere radiation budgets in Figure 2b).

SSTs and atmospheric circulation along the equator are shown in Figure 8. While warm-pool temperatures in the western Pacific remain near 28°C within the early Pliocene experiment, temperatures in the middle of the eastern Pacific cold tongue have warmed by 4°C (Figure 8d versus Figure 8b). In response to the weakening of the east-west temperature gradient, and the ensuing coupled ocean-atmosphere feedbacks, zonal atmospheric Walker circulation within the Pacific basin is substantially reduced within the Pliocene experiment (Figure 8c versus Figure 8a). This reduction results in a smaller east-west thermocline slope along the equator, which can be inferred from Figure 5b, and is consistent with reconstructions based on oxygen isotopes and planktonic foraminiferal assemblages [*Chaisson and Ravelo*, 2000; *Chaisson*, 1995].

Figure 9a depicts the changes in precipitation that result from these large-scale changes in atmospheric circulation. As the warm pool has expanded poleward and eastward, convection has spread out with it, distributing precipitation over a larger area and decreasing it within the western tropical Pacific. Consistent with a weakening in Hadley circulation, precipitation in the Pliocene experiment is reduced in regions of uplift corresponding with the modern ITCZ and is enhanced within regions where present-day rainfall is suppressed by subsidence. Convection in the Pliocene experiment shifts eastward, occurring more uniformly across the tropical Pacific basin in response to the weaker zonal SST gradient, with weaker Walker circulation resulting in enhance rainfall within the eastern equatorial Pacific.

As part of precipitation changes, the Pliocene simulation predicts a weakening of the South Asian monsoon, and an increase in precipitation over East Africa, in part, related to the reduction in the zonal SST gradient in the Arabian sea (Figure 3c). Other regions with increased precipitation include Southern Africa, Australia, and Southern California. In all of these regions, dominated by deserts or semiarid regions

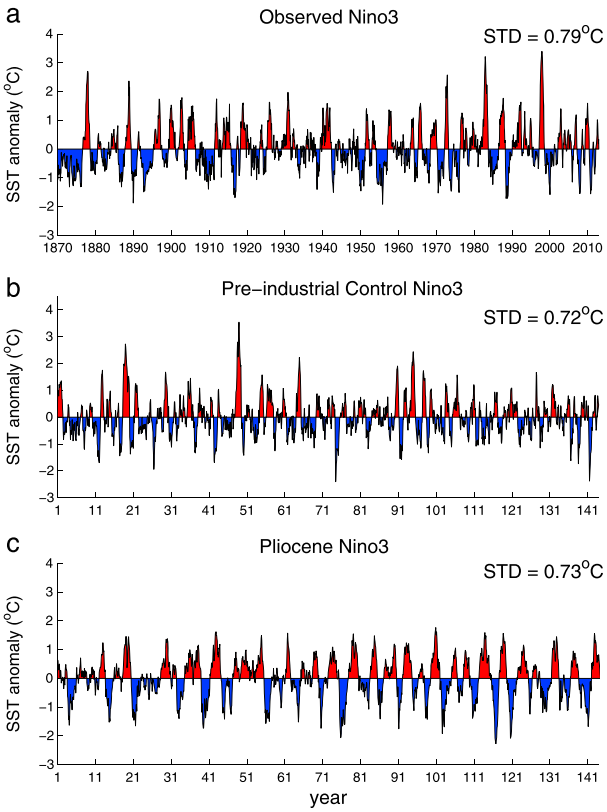

Figure 11. Niño3 SST anomalies for (a) observations and the (b) preindustrial control and (c) early Pliocene experiments. The standard deviations of the three records are 0.79°C, 0.72°C, and 0.73°C, respectively. Same original data were used in Figure 10.

at present, available observational evidence suggests wetter conditions during the Pliocene [*Molnar and Cane*, 2007; *Salzmann et al.*, 2009].

Changes in atmospheric circulation also lead to changes in surface wind stress over the ocean (Figure 9b). For example, the weaker Hadley circulation results in weaker trades. The weakening of atmospheric subsidence in the Hadley cell leads to a weakening of the high surface pressure regions in the subtropics (subtropical highs) and of the associated anticyclonic flow. The result is a weakening of the alongshore winds that support coastal upwelling along the eastern basin boundaries—a mechanism which could have supported the much warmer coastal upwelling regions during the Pliocene [*Herbert and Schuffert*, 1998; *LaRiviere et al.*, 2012; *Marlow et al.*, 2000; *Dekens et al.*, 2007; *Brierley et al.*, 2009].

The decreased wind stress between 35° and 50° and enhanced wind stress poleward is consistent with a poleward shift in midlatitude storm tracks due to the amplified high-latitude warming seen in the early Pliocene experiment, a robust result emerging from global warming studies [e.g., *Chen and Held*, 2007]. This poleward shift of the westerlies during the Pliocene is consistent with observed shifts in marine productivity [*Lawrence et al.*, 2013]. High marine biological export productivity in the high-latitude regions in the North Pacific, Atlantic, and Southern Ocean during the Pliocene declined with the intensification of Northern Hemisphere glaciation. *Lawrence et al.* [2013] suggest that productivity was higher in the high-latitude regions during the Pliocene because the westerly winds were situated further poleward and that it decreased as the maxima in westerly winds migrated equatorward—shifting the region of maximum Ekman divergence and hence the upwelling-induced nutrient supply equatorward.

5. ENSO During the Pliocene

Proxy evidence suggests that interannual climate variability associated with the El Niño-Southern Oscillation persisted during the Pliocene [*Watanabe et al.*, 2011; *Scroxton et al.*, 2011] despite the fact that the mean state was characterized by a reduced east-west SST gradient. In this section we investigate the impact that the structural change in the background climate state between the preindustrial control and Pliocene experiments has on interannual SST variability within the equatorial Pacific. For comparison, we use observations in the tropical Pacific over the last 143 years (January 1870 to December 2012) and the last 143 years of the preindustrial control and Pliocene simulations.

The spatial structure of the variance of monthly interannual SST anomalies is generally similar between the preindustrial control simulation and the observations (Figures 10a and 10b); regions where the standard deviation exceeds 0.8°C occur within both the central and eastern Pacific, although variability within the central Pacific is somewhat stronger and extends further westward in the control. The overall character of Niño3 SST variations, indicative of ENSO, is also rather similar between the observations and the control (Figures 11a and 11b).

Looking now at the Pliocene simulation reveals several important points. First of all, a robust ENSO-like interannual variability seen in the Niño3 index and SST spatial variance still persists (Figures 10c and 11c), even though the zonal SST gradient has been reduced from 6.5°C to about 2°C. In fact, the Niño3 region still provides the best description of the interannual variability. Moreover, the standard deviations for each of the three time series are statistically indistinguishable: 0.79°C (observations), 0.72°C (Control), and 0.73°C (Pliocene). ENSO variability within the Pliocene simulation has, however, become slightly skewed toward stronger cold events. As discussed in more detail below, the reduced east-west SST gradient and warmer climatological SSTs in the east preclude very strong El Niño but not La Niña events.

It is important to note, however, that there is substantial decadal and longer-term variations, driven purely by internal variability, affecting the above statistics. For example, if one considers different 30 year segments within each of the time series in Figure 11, the standard deviation (SD) of the Niño3 index varies between 0.61°C and 0.98°C within the observations, 0.55°C and 0.81°C for the pre-industrial control, and 0.61°C and 0.87°C for the Pliocene simulation. Similar variations are found if one chooses different 143 year slices within the numerical experiments. These results are consistent with long numerical simulations by other climate models [e.g., *Wittenberg*, 2009] and highlight that caution is required when drawing conclusions based on short-proxy time series.

Despite the aforementioned similarities between the simulated ENSO in the Pliocene and control experiments, there are several important differences. Because of a smaller cold tongue, interannual variability of SST in the Pliocene simulation is confined solely to the eastern Pacific (with SD $\geq$ 0.8°C). The reduction of the mean zonal SST gradient also puts a cap on strong warm events, so that extreme El Niño events (positive Niño3 SST anomalies exceeding 2°C) disappear within the Pliocene simulation. This is because the maximum possible temperature, that of surface waters in the warm pool, is now only some 2°C warmer than the climatological SST for the Niño3 region. In contrast to El Niño events, strong La Niña events become more frequent. Finally, the dominant period of ENSO, as estimated from spectral analyses of the time series, shifts from about 3 to 5 years between the control and Pliocene experiments and the oscillation becomes more regular as a larger percentage of the total variance is concentrated within its spectral peak.

While an in-depth analysis of the system stability and feedbacks sustaining ENSO within the Pliocene experiment is beyond the scope of this study, these results are generally consistent with those emanating from a recent sensitivity study by *Manucharyan and Fedorov* [2014] who systematically investigate the sensitivity of ENSO variability to changes in the mean zonal SST gradient. The authors also use CESM but employ a different approach to change tropical climate. Namely, they modify upper ocean vertical mixing in the extratropics—higher mixing leads to warmer temperatures in the eastern equatorial Pacific. The central finding of *Manucharyan and Fedorov* [2014] is that ENSO remains surprisingly robust. Reducing the mean east-west SST gradient from 6°C to 1°C over a series of experiments decreases the amplitude of ENSO (defined as the standard deviation of the Niño3 index) by 30–40%, but the spectral peak remains statistically significant for very small values of the SST gradient. They also find a slight increase in the period of ENSO, from 3 to 4 years, for smaller gradients. Having evaluated the magnitude of the ocean-atmosphere feedbacks that control ENSO stability, *Manucharyan and Fedorov* [2014] ascribe the robustness of ENSO to the fact that the growth/decay rates of the ENSO natural mode stay nearly constant across different climates. These rates remain approximately constant due to compensating effects associated with the reorganization of the atmospheric Walker circulation in response to changes in the mean surface temperature gradient.

6. Discussion and Conclusion

A reduced meridional albedo gradient could have supported Pliocene warmth as well as the weak SST gradients revealed by proxy data for the early Pliocene. More specifically, our results suggest that a roughly 0.04 decrease in extratropical albedo and a 0.06 increase in tropical albedo may be necessary to maintain the structurally different sea surface temperature structure of the early Pliocene.

Lower extratropical cloud albedo increases the amount of shortwave radiation reaching the ocean surface raising the temperature of water subducted in the downwelling regions of the subtropical, wind-driven overturning circulation. This extratropical warming translates into the upwelling of warmer subsurface water in the equatorial and coastal upwelling regions. With the disappearance of cold eastern basin SSTs, tropical atmospheric convection is no longer confined to the west and expands eastward across the basin. Increased tropical Pacific albedo acts to decrease the heat flux into the tropical Pacific ocean ensuring

that western Pacific warm-pool SSTs remain relatively constant. The extent of warming in the warm pool depends on both the reduction in extratropical albedo and the extent to which tropical albedo is increased.

The warming of SSTs in the east but not the west decreases the zonal SST gradient. Consequently, the mean intensity of the atmospheric Walker circulation and the easterly trade winds together with the zonal slope of the equatorial thermocline all decrease in response to a reduction in the meridional albedo gradient. Similarly, the strength of the Hadley circulation decreases due to a corresponding reduction in the meridional SST gradient.

This weakening of the Walker and Hadley cells strongly affects surface winds and precipitation. Precipitation is reduced in regions of large-scale ascent and enhanced in regions of descent, generally resulting in wetter conditions over present-day deserts and semiarid regions. The reduced subsidence in the Hadley cells results in the weakening of the Subtropical Highs and atmospheric anticyclonic circulation over the eastern halves of the ocean basins, which in turn leads to a weakening of the alongshore winds driving coastal upwelling. This effect would have contributed to the exceptional warmth of the coastal upwelling regions suggested by proxy data for the Pliocene (as mentioned in section 3, we hypothesize that one of the reasons that the Pliocene simulation does not reproduce the full extent of this warming despite capturing the reduction in alongshore wind is due to its insufficient bathymetric resolution). Poleward of the subtropics, the amplified high-latitude warming in the Pliocene experiment is associated with a poleward shift in midlatitude storm tracks.

Other robust results of this study concern the thermal structure of the upper ocean. The distinctly different global SST pattern within the early Pliocene experiment is supported by a change in the thermal structure of the upper ocean. Thermocline waters have warmed resulting in a warmer thermal stratification and weaker stratification across the equatorial thermocline.

The climate maintained by the albedo changes imposed in the Pliocene experiment agrees well with the paleoclimate evidence available for the early Pliocene in several ways. The simulation has managed to capture the amplified warming of SSTs seen within proxy data from the middle to high latitudes [*Lawrence et al.*, 2010; *LaRiviere et al.*, 2012], subtropical coastal upwelling regions [*Herbert and Schuffert*, 1998; *LaRiviere et al.*, 2012; *Marlow et al.*, 2000; *Dekens et al.*, 2007; *Brierley et al.*, 2009], and the eastern equatorial Pacific cold tongue [*Wara et al.*, 2005; *Fedorov et al.*, 2006; *Dekens et al.*, 2007; *Lawrence et al.*, 2006; *Ford et al.*, 2012]. This structural change in the large-scale SST field is supported by changes in the thermal structure of the upper ocean that appears to be consistent with observed subsurface temperature changes in the eastern Pacific [*Ford et al.*, 2012; *Steph et al.*, 2010, 2006].

With warm-pool temperatures remaining relatively constant [*Wara et al.*, 2005; *Karas et al.*, 2009; *Pagani et al.*, 2010; *Karas et al.*, 2011b] and cold tongue temperatures substantially warmer, the simulated reduction in the east-west SST gradient, reduced easterly trades and zonal thermocline slope in the Pliocene experiment, is consistent with several paleoclimate studies [*Chaisson*, 1995; *Chaisson and Ravelo*, 2000; *Wara et al.*, 2005; *Fedorov et al.*, 2006; *Ravelo et al.*, 2006; *Brierley et al.*, 2009; *Fedorov et al.*, 2013]. Moreover, the weak meridional and zonal SST gradients and the associated weakening of the Walker and Hadley cells maintain large-scale precipitation changes that are qualitatively consistent with Pliocene reconstructions [*Salzmann et al.*, 2009; *Molnar and Cane*, 2007].

Note that it has been suggested that tropical SST estimates for the Pliocene based on Mg/Ca should be corrected (increased) due to secular changes in the Mg/Ca ratio of seawater [e.g., *Medina-Elizalde et al.*, 2008; *Zhang et al.*, 2014]. The consistency between proxy data of different types and in different locations (Figure 3) suggests that this correction should not exceed 1°C, which would slightly improve the overall data/model agreement in the Indo-Pacific warm pool. However, a greater correction would make some of the proxy data inconsistent: for example, if a correction larger than 1°C is applied to eastern equatorial Pacific site 847, the Mg/Ca temperature estimates at this site would be much warmer than concomitant alkenone temperature estimates.

Finally, our fully coupled Pliocene-like simulation indicates that there is no inconsistency between proxy evidence suggesting that interannual climate variability associated with the El Niño-Southern Oscillation persisted during the Pliocene [*Watanabe et al.*, 2011; *Scroxton et al.*, 2011] and the fact that the mean state was characterized by permanent El Niño-like conditions. Indeed, despite a much weaker mean east-west SST gradient and thermocline slope, interannual SST variability in the eastern Pacific associated with the El Niño

Southern Oscillation phenomenon persists within the early Pliocene experiment. Relative to present-day ENSO statistics, the interannual SST variability is weaker in magnitude in the central Pacific but similar in the eastern Pacific. The standard deviation of Niño3 SST remains comparable with modern values; at the same time the number of strong El Niño events decreases, while the number of strong La Niño events increases. The dominant period of ENSO lengthens albeit slightly, and the oscillation becomes more regular.

Although certain aspects of these ENSO changes within a Pliocene-like background state may be model dependent, the main result indicating that ENSO persists in within the coupled ocean-atmosphere system even once the mean east-west SST gradient has been substantially reduced, is consistent with the sensitivity study of *Manucharyan and Fedorov* [2014]. While both studies use the same climate model (CESM), they differ in the mechanism employed to maintain a reduced east-west SST gradient along the equator, providing confidence in the result that the ENSO should persist for weak (but nonzero) zonal SST gradients. Further studies with different GCMs are, however, necessary to rigorously test this finding.

The feasibility and possible cause of the albedo changes required within our simulations to shift between modern and early Pliocene conditions remain open questions. There are two possible scenarios that could give rise to these albedo changes: (1) cloud feedbacks, currently unresolved by coupled climate models in response to CO_2-induced warming during the Pliocene and (2) the different vegetation, orography, and ice sheets of the Pliocene [e.g., *Lunt et al.*, 2010] could have supported a different composition of atmospheric aerosols [e.g., *Unger and Yue*, 2014] and therefore cloud condensation and ice nuclei. For example, previous studies have shown evidence that levels of dust, an important ice nuclei [*Murray et al.*, 2012], were substantially lower 4 Ma [*Martínez-Garcia et al.*, 2011].

Our understanding of changes in cloud radiative forcing within paleoclimates in general is uncertain [*Rohling et al.*, 2012]. A recent study by *Kiehl and Shields* [2013], exploring the general sensitivity of the Paleocene-Eocene Thermal Maximum climate state to changes in cloud microphysical properties, assumes that all cloud condensation nuclie values were closer to those observed in present-day pristine conditions. While the associated change in cloud albedo is not explicitly mentioned, the induced changes in cloud properties yield a 7 to 9°C warming at the poles. *Kump and Pollard* [2008] suggest that reduced cloud condensation nuclei during the warm equable climate of the Cretaceous could have supported less extensive and optically thinner clouds reducing planetary albedo from 0.30 to 0.24. This reduction in cloud albedo is required in addition to elevated CO_2 levels to produce the extreme high-latitude warmth implied by proxy data for the middle Cretaceous. Furthermore, high-latitude cloud feedbacks due to longwave trapping by both convective clouds [*Abbot and Tziperman*, 2008a, 2008b] and polar stratospheric clouds [*Sloan and Pollard*, 1998; *Kirk-Davidoff et al.*, 2002] have been put forward to explain equable climates.

Even if particular details of the proposed mechanism for sustaining Pliocene climate—changes in meridional distribution of cloud albed—turn out to be incorrect, the major conclusions of this study will still remain valid. The simulated global SST pattern within the Pliocene experiment is associated with reduced poleward atmospheric as well as oceanic heat transport (Figure 7). This result suggests that the required equator to pole heat transport of the coupled ocean-atmosphere system has to be reduced to support Pliocene-like conditions. Such a change in heat transport requires a structurally different TOA radiation budget relative to today, a budget where outgoing radiation is balanced more locally by incoming radiation. This can be achieved in one of two ways—either the intensity of outgoing longwave radiation or the reflection of incoming shortwave radiation must change, so that these two variables become more locally balanced. This study has focused on the later mechanism. The main impact of the imposed changes in radiative forcing, regardless of the actual mechanism, is to maintain a reduced meridional SST gradient. In fact, a major corollary of this study is that replicating the mean meridional temperature gradient correctly is key to reproducing the geographical patterns of Pliocene warmth.

Acknowledgments

This research is supported by grants from the Department of Energy Office of Science (DE-SC0007037), NSF (AGS-1405272), and the David and Lucile Packard Foundation. The CESM project is supported by the National Science Foundation and the Department of Energy Office of Science. Computations were performed at the Yale University Faculty of Arts and Sciences High Performance Computing Center. The model data used in this study will be made available in the Paleoclimatology Modeling section of NOAA's National Climate Data Center and are also available on request. We thank Chris Brierley and Brian Dobbins for their advice in setting up the CESM simulations, as well as George Philander, Christina Ravelo, and Heather Ford for insightful discussions on this work. Finally, we would like to thank the reviewers of this paper for their very constructive feedback.

References

Abbot, D., and E. Tziperman (2008a), Sea ice, high-latitude convection, and equable climates, *Geophys. Res. Letters.*, *35*(3), L03702, doi:10.1029/2007GL032286.

Abbot, D., and E. Tziperman (2008b), A high-latitude convective cloud feedback and equable climates, *Q. J. R. Meteorol. Soc.*, *134*(630), 165–185.

Barreiro, M., and S. Philander (2008), Response of the tropical Pacific to changes in extratropical clouds, *Clim. Dyn.*, *31*(6), 713–729.

Bjerknes, J. (1969), Atmospheric teleconnections from the equatorial Pacific, *Mon. Weather Rev.*, *97*, 163–172.

Boccaletti, G., R. C. Pacanowski, S. G. H. Philander, and A. V. Fedorov (2004), The thermal structure of the upper ocean, *J. Phys. Oceanogr.*, *34*, 888–902.

Brierley, C., and A. Fedorov (2010), Relative importance of meridional and zonal sea surface temperature gradients for the onset of the ice ages and Pliocene-Pleistocene climate evolution, *Paleoceanography*, *25*(2), PA2214, doi:10.1029/2009PA001809.
Brierley, C. M., A. V. Fedorov, Z. Liu, T. D. Herbert, K. T. Lawrence, and J. P. LaRiviere (2009), Greatly expanded tropical warm pool and weakened hadley circulation in the early Pliocene, *Science*, *323*, 1714–1718, doi:10.1126/science.1167625.
Burls, N., and A. Fedorov (2014), What controls the mean east-west sea surface temperature gradient in the equatorial Pacific: The role of cloud albedo, *J. Clim.*, *27*(7), 2757–2778.
Cane, M., and P. Molnar (2001), Closing of the Indonesian seaway as a precursor to east African aridification around 3–4 million years ago, *Nature*, *411*(6834), 157–162.
Chaisson, W. (1995), Planktonic foraminiferal assemblages and paleoceanographic change in the trans-tropical Pacific Ocean: A comparison of west (Leg 130) an east (Leg 138), latest Miocene to Pleistocene, in *Proceedings of the Ocean Drilling Program. Scientific Results*, vol. 138, edited by N. G. Pisias et al., pp. 555–597, Ocean Drilling Program, College Station, Tex.
Chaisson, W., and A. Ravelo (2000), Pliocene development of the east-west hydrographic gradient in the equatorial Pacific, *Paleoceanography*, *15*(5), 497–505.
Chen, G., and I. M. Held (2007), Phase speed spectra and the recent poleward shift of Southern Hemisphere surface westerlies, *Geophys. Res. Lett.*, *34*, L21805, doi:10.1029/2007GL031200.
Dekens, P., A. Ravelo, and M. McCarthy (2007), Warm upwelling regions in the Pliocene warm period, PA3211, doi:10.1029/2006PA001394.
Dowsett, H., et al. (2012), Assessing confidence in Pliocene sea surface temperatures to evaluate predictive models, *Nat. Clim. Change*, *2*(5), 365–371.
Dowsett, H., et al. (2013), Sea surface temperature of the mid-Piacenzian Ocean: A data-model comparison, *Sci. Rep.*, *3*, 2013.
Fedorov, A., R. Pacanowski, S. Philander, and G. Boccaletti (2004), The effect of salinity on the wind-driven circulation and the thermal structure of the upper ocean, *J. Phys. Oceanogr.*, *34*(9), 1949–1966.
Fedorov, A., C. Brierley, and K. Emanuel (2010), Tropical cyclones and permanent El Niño in the early Pliocene epoch, *Nature*, *463*(7284), 1066–1070.
Fedorov, A., C. M. Brierley, K. T. Lawrence, Z. Liu, P. S. Dekens, and A. Ravelo (2013), Patterns and mechanisms of early Pliocene warmth, *Nature*, *496*, 43–49.
Fedorov, A. V., P. S. Dekens, M. McCarthy, A. C. Ravelo, P. B. de Menocal, M. Barreiro, R. C. Pacanowski, and S. G. Philander (2006), The Pliocene paradox (mechanisms for a permanent El Niño), *Science*, *312*, 1485–1489, doi:10.1126/science.1122666.
Ford, H., A. Ravelo, and S. Hovan (2012), A deep eastern equatorial pacific thermocline during the early Pliocene warm period, *Earth Planet. Sci. Lett.*, *355*, 152–161.
Gu, D., and S. G. H. Philander (1997), Interdecadal climate fluctuations that depend on exchanges between the tropics and extratropics, *Science*, *5301*, 805–807.
Haug, G., R. Tiedemann, R. Zahn, and A. Ravelo (2001), Role of Panama uplift on oceanic freshwater balance, *Geology*, *29*(3), 207–210.
Haywood, A., and P. Valdes (2004), Modelling Pliocene warmth: contribution of atmosphere, oceans and cryosphere, *Earth Planet. Sci. Lett.*, *218*(3), 363–377.
Haywood, A., P. Valdes, and V. Peck (2007), A permanent El Niño-like state during the Pliocene?, *Paleoceanography*, *22*(1), PA1213, doi:10.1029/2006PA001323.
Herbert, T., and J. Schuffert (1998), Alkenone unsaturation estimates of late Miocene through late Pliocene sea-surface temperatures at site 958, *Proc. Ocean Drill. Program Sci. Results*, *159T*, 17–21.
Karas, C., D. Nürnberg, A. Gupta, R. Tiedemann, K. Mohan, and T. Bickert (2009), Mid-Pliocene climate change amplified by a switch in Indonesian subsurface throughflow, *Nat. Geosci.*, *2*(6), 434–438.
Karas, C., D. Nürnberg, R. Tiedemann, and D. Garbe-Schönberg (2011a), Pliocene climate change of the Southwest Pacific and the impact of ocean gateways, *Earth Planet. Sci. Lett.*, *301*(1), 117–124.
Karas, C., D. Nürnberg, R. Tiedemann, and D. Garbe-Schönberg (2011b), Pliocene Indonesian throughflow and Leeuwin current dynamics: Implications for Indian Ocean polar heat flux, *Paleoceanography*, *26*(2), PA2217, doi:10.1029/2010PA001949.
Kiehl, J., and C. Shields (2013), Sensitivity of the Paleocene-Eocene thermal maximum climate to cloud properties, *Phil. Trans. R. Soc. A.*, *371*(2001), 20,130,093.
Kirk-Davidoff, D., D. Schrag, and J. Anderson (2002), On the feedback of stratospheric clouds on polar climate, *Geophys. Res. Lett.*, *29*(11), 51-1–51-4, doi:10.1029/2002GL014659.
Kump, L., and D. Pollard (2008), Amplification of Cretaceous warmth by biological cloud feedbacks, *Science*, *320*(5873), 195–195.
LaRiviere, J., A. Ravelo, A. Crimmins, P. Dekens, H. Ford, M. Lyle, and M. Wara (2012), Late Miocene decoupling of oceanic warmth and atmospheric carbon dioxide forcing, *Nature*, *486*(7401), 97–100.
Lawrence, K., Z. Liu, and T. Herbert (2006), Evolution of the eastern tropical Pacific through Plio-Pleistocene glaciation, *Science*, *312*(5770), 79–83.
Lawrence, K., T. Herbert, C. Brown, M. Raymo, and A. Haywood (2009), High-amplitude variations in North Atlantic sea surface temperature during the early Pliocene warm period, *Paleoceanography*, *24*(2), PA2218, doi:10.1029/2008PA001669.
Lawrence, K., S. Sosdian, H. White, and Y. Rosenthal (2010), North Atlantic climate evolution through the Plio-Pleistocene climate transitions, *Earth Planet. Sci. Lett.*, *300*(3), 329–342.
Lawrence, K., D. Sigman, T. Herbert, C. Riihimaki, C. Bolton, A. Martinez-Garcia, A. Rosell-Mele, and G. Haug (2013), Time-transgressive North Atlantic productivity changes upon Northern Hemisphere glaciation, *Paleoceanography*, *28*(4), 740–751, doi:10.1002/2013PA002546.
Liu, Z., and T. Herbert (2004), High-latitude influence on the eastern equatorial Pacific climate in the early Pleistocene epoch, *Nature*, *427*(6976), 720–723.
Lunt, D., A. Haywood, G. Schmidt, U. Salzmann, P. Valdes, and H. Dowsett (2010), Earth system sensitivity inferred from Pliocene modelling and data, *Nat. Geosci.*, *3*(1), 60–64.
Lunt, D. J., P. J. Valdes, A. Haywood, and I. C. Rutt (2008), Closure of the Panama Seaway during the Pliocene: Implications for climate and Northern Hemisphere glaciation, *Clim. Dyn.*, *30*(1), 1–18.
Maier-Reimer, E., U. Mikolajewicz, and T. Crowley (1990), Ocean general circulation model sensitivity experiment with an open Central American Isthmus, *Paleoceanography*, *5*(3), 349–366.
Manabe, S., and R. Stouffer (1988), Two stable equilibria of a coupled ocean-atmosphere model, *J. Clim.*, *1*(9), 841–866.
Manucharyan, G., and A. Fedorov (2014), Robust ENSO across climates with a wide range of mean east-west SST gradients, *J. Clim.*, *27*, 5836–5850, doi:10.1175/JCLI-D-13-00759.1.
Marlow, J., C. Lange, G. Wefer, and A. Rosell-Melé (2000), Upwelling intensification as part of the Pliocene-Pleistocene climate transition, *Science*, *290*(5500), 2288–2291.

Martínez-Garcia, A., A. Rosell-Melé, S. L. Jaccard, W. Geibert, D. M. Sigman, and G. H. Haug (2011), Southern Ocean dust-climate coupling over the past four million years, *Nature*, *476*(7360), 312–315.
McCreary, J. P. J., and P. Lu (1994), Interaction between the subtropical and the equatorial oceans: The subtropical cell, *J. Phys. Oceanogr.*, *24*, 466–497.
Medina-Elizalde, M., D. Lea, and M. Fantle (2008), Implications of seawater Mg/Ca variability for Plio-Pleistocene tropical climate reconstruction, *Earth Planet. Sci. Lett.*, *269*(3), 585–595.
Mohtadi, M., D. Oppo, A. Lückge, R. DePol-Holz, S. Steinke, J. Groeneveld, N. Hemme, and D. Hebbeln (2011), Reconstructing the thermal structure of the upper ocean: Insights from planktic foraminifera shell chemistry and alkenones in modern sediments of the tropical eastern Indian Ocean, *Paleoceanography*, *26*(3), PA3219, doi:10.1029/2011PA002132.
Molnar, P. (2008), Closing of the Central American seaway and the ice age: A critical review, *Paleoceanography*, *23*(2), PA2201, doi:10.1029/2007PA001574.
Molnar, P., and M. A. Cane (2007), Early Pliocene (pre-Ice Age) El Niño-like global climate: Which El Niño?, *Geosphere*, *3*(5), 337–365.
Murray, B., D. O'Sullivan, J. Atkinson, and M. Webb (2012), Ice nucleation by particles immersed in supercooled cloud droplets, *Chem. Soc. Rev.*, *41*(19), 6519–6554.
Pagani, M., Z. Liu, J. LaRiviere, and A. Ravelo (2010), High Earth-system climate sensitivity determined from Pliocene carbon dioxide concentrations, *Nat. Geosci.*, *3*(1), 27–30.
Philander, S., and A. Fedorov (2003), Role of tropics in changing the response to Milankovich forcing some three million years ago, *Paleoceanography*, *18*(2), 1045, doi:10.1029/2002PA000837.
Ravelo, A., P. Dekens, and M. McCarthy (2006), Evidence for El Niño-like conditions during the Pliocene, *GSA Today*, *16*(3), 4–11.
Rayner, N. A., D. E. Parker, E. B. Horton, C. K. Folland, L. V. Alexander, D. P. Rowell, E. C. Kent, and A. Kaplan (2003), Global analyses of sea surface temperature, sea ice, and night marine air temperature since the late nineteenth century, *J. Geophys. Res.*, *108*(D14), 4407, doi:10.1029/2002JD002670.
Rohling, E., et al. (2012), Making sense of palaeoclimate sensitivity, *Nature*, *491*(7426), 683–691.
Salzmann, U., A. Haywood, and D. Lunt (2009), The past is a guide to the future? Comparing middle Pliocene vegetation with predicted biome distributions for the twenty-first century, *Philos. Trans. R. Soc. A*, *367*(1886), 189–204.
Scroxton, N., S. Bonham, R. Rickaby, S. Lawrence, M. Hermoso, and A. Haywood (2011), Persistent El Niño-Southern Oscillation variation during the Pliocene epoch, *Paleoceanography*, *26*(2), PA2215, doi:10.1029/2010PA002097.
Seki, O., D. Schmidt, S. Schouten, E. Hopmans, J. S. Sinninghe, and R. D. Pancost (2012), Paleoceanographic changes in the Eastern equatorial Pacific over the last 10 Myr, *Paleoceanography*, *27*(3), PA3224, doi:10.1029/2011PA002158.
Sloan, L. C., and D. Pollard (1998), Polar stratospheric clouds: A high latitude warming mechanism in an ancient greenhouse world, *Geophys. Res. Lett.*, *25*(18), 3517–3520.
Steph, S., R. Tiedemann, J. Groeneveld, A. Sturm, and D. Nürnberg (2006), Pliocene changes in tropical east Pacific upper ocean stratification: Response to tropical gateways?, in *Proceedings of the Ocean Drilling Program: Scientific Results*, vol. 202, edited by R. Tiedemann et al., pp. 1–51, Ocean Drilling Program, College Station, Tex.
Steph, S., R. Tiedemann, M. Prange, J. Groeneveld, M. Schulz, A. Timmermann, D. Nürnberg, C. Rühlemann, C. Saukel, and G. H. Haug (2010), Early Pliocene increase in thermohaline overturning: A precondition for the development of the modern equatorial Pacific cold tongue, *Paleoceanography*, *25*(2), PA2202, doi:10.1029/2008PA001645.
Tziperman, E., and B. Farrell (2009), Pliocene equatorial temperature: Lessons from atmospheric superrotation, *Paleoceanography*, *24*(1), PA1101, doi:10.1029/2008PA001652.
Unger, N., and X. Yue (2014), Strong chemistry-climate feedbacks in the Pliocene, *Geophys. Res. Lett.*, *41*, 527–533, doi:10.1002/2013GL058773.
Wara, M. W., A. C. Ravelo, and D. L. Margaret (2005), Permanent El Niño-like conditions during the Pliocene warm period, *Science*, *309*, 758–761, doi:10.1126/science.1112596.
Watanabe, T., et al. (2011), Permanent El Niño during the Pliocene warm period not supported by coral evidence, *Nature*, *471*(7337), 209–211.
Wittenberg, A. (2009), Are historical records sufficient to constrain ENSO simulations?, *Geophys. Res. Lett.*, *36*(12), L12702, doi:10.1029/2009GL038710.
Zhang, X., et al. (2012), Changes in equatorial Pacific thermocline depth in response to Panamanian seaway closure: Insights from a multi-model study, *Earth Planet. Sci. Lett.*, *317*, 76–84.
Zhang, Y. G., M. Pagani, and Z. Liu (2014), A 12-million-year temperature history of the tropical Pacific ocean, *Science*, *344*(6179), 84–87.